Mathematical Geology, Vol. 33, No. 3, 2001

Scale Invariances in the Morphology and Evolution of Braided Rivers[1]

Efi Foufoula-Georgiou[2] and Victor Sapozhnikov[2,3]

This paper presents an overview and synthesis of an extensive research effort to characterize and quantify scale invariances in the morphology and evolution of braided rivers. Braided rivers were shown to exhibit anisotropic spatial scaling (self-affinity) in their morphology, implying a statistical scale invariance under appropriate rescaling of the axes along and perpendicular to the main direction of flow. The scaling exponents were found similar in rivers of diverse flow regimes, slopes, types of bed material and braid plain widths, indicating the presence of universal features in the underlying mechanisms responsible for the formation of their spatial structure. In regions where predominant geologic controls or predominant flow paths were present, no spatial scaling was found. Regarding their spatiotemporal evolution, braided rivers were found to exhibit dynamic scaling, implying that a smaller part of a braided river evolves identically to a larger one provided that space and time are appropriately normalized. Based on these findings, and some additional analysis of experimental rivers as they approach equilibrium, it was concluded that the mechanism bringing braided rivers to a state where they show spatial and temporal scaling is self-organized criticality and inferences about the physical mechanisms of self-organization were suggested.

KEY WORDS: self-affinity, dynamic scaling, self-organized criticality.

INTRODUCTION

Braided rivers consist of numerous alluvial channels that divide and rejoin around bars and islands, forming an intertwining structure that resembles a braid. They prevail in mountainous and glacial regions, and are highly dynamic systems characterized by intensive erosion, sediment transport and deposition, and frequent channel shifting. The alluvial deposits of braided rivers are important reservoirs of water, oil, gas, coal, sand, gravel and heavy minerals.

Considerable research on braided rivers has focused on understanding the small-scale processes such as flow and sediment flux around an individual channel

[1]Received 15 July 1999; accepted 1 February 2000.

[2]St. Anthony Falls Laboratory, Department of Civil Engineering, University of Minnesota, Minneapolis, Minnesota 55414. e-mail: efi@tc.umn.edu

[3]Present address: Seagate Technology, Minneapolis, Minnesota.

0882-8121/01/0400-0273$19.50/1

bar or confluence (Ashmore and Parker, 1983; Ashmore and others, 1992; Best, 1986; Bristow, Best, and Roy 1993; Mosley, 1976, 1977; Robert, 1993). Most recently, efforts have also been directed on understanding the mechanics and hydrology of the entire braided river system (e.g., Murray and Paola, 1994; Smith and others, 1995, 1996; see also the early study of Howard, Keetch, and Vincent, 1970). Understanding the overall behavior and dynamics of a braided stream system is needed for a variety of applications such as the quantification of the ecological effects of migrating channels at a range of scales, the optimal harvesting of rich mineral deposits left on inactive bars and banks, and even the statistical prediction of extreme channel migration for planning bridge and waterway passages.

In the past five years, an extensive theoretical and experimental effort was undertaken in our group focusing on characterizing the statistical spatiotemporal structure of fully developed braided rivers in a variety of geological and hydrological regimes and at a range of spatial and temporal scales (Sapozhnikov and Foufoula-Georgiou, 1996a,b; Nykanen, Foufoula-Georgiou, and Sapozhnikov, 1998; Foufoula-Georgiou and Sapozhnikov, 1998; Sapozhnikov and Foufoula-Georgiou, 1997; Sapozhnikov and others, 1998; Sapozhnikov and Foufoula-Georgiou, 1999). The underlying theme of this effort was the realization that there are fundamental statistical similarities between small and larger parts of a braided river and between one braided river and another both in terms of static morphology and evolutionary dynamics. If these similarities were quantified, parsimonious statistical descriptions of the planform geometry and evolution of braided rivers at a range of scales could result. Also, long-term rare changes in a system could be statistically predicted from shorter-term frequent changes for which data were available. These ideas motivated our goal to seek quantitative descriptions of scale invariances in braided rivers that had been widely recognized in the past by geomorphologists (e.g., see Bristow and Best, 1993) but had not been quantified in any rigorous manner.

At first glance, the spatial structure of a large part of a braided river and its structure at the level of channels appear to have some kind of similarity. For example, Figure 1 illustrates that a small part of the river looks statistically similar to a larger part under appropriate rescaling of the spatial coordinates. Moreover, visual comparison of the spatial patterns of different braided rivers renders it impossible to determine the natural scale of each of the systems, e.g., it might not be possible to tell with confidence whether the braid plain width of a river is of the order of 1 or 10 or 100 km by just looking at a picture of it. This is illustrated in Figure 2, which shows digitized images of three braided rivers: the Brahmaputra River in Bangladesh, and the Aichilik and Hulahula Rivers in Alaska. These rivers have different natural scales (0.5 to 15 km in braid plain widths and 6.4 to 200 km in length of analyzed sections) and different slopes and bed materials (e.g., see Table 1), yet it is difficult to discern these differences

Table 1. Hydrologic and Geomorphologic Characteristics of the Studied Rivers

	Brahmaputra	Aichilik	Hulahula
Reach width, km	15	0.5	0.7
Reach length, km	200	6.4	20
Mean channel depth, m	5	1	1
Slope	0.000077	0.001	0.0007
Braiding index[a]	3.8	6.8	5.2
Predominant type of the bed material	Sand	Gravel	Gravel

[a] The braiding index (BI) for each river was computed as the average number of channels in cross sections of the photo image of the river.

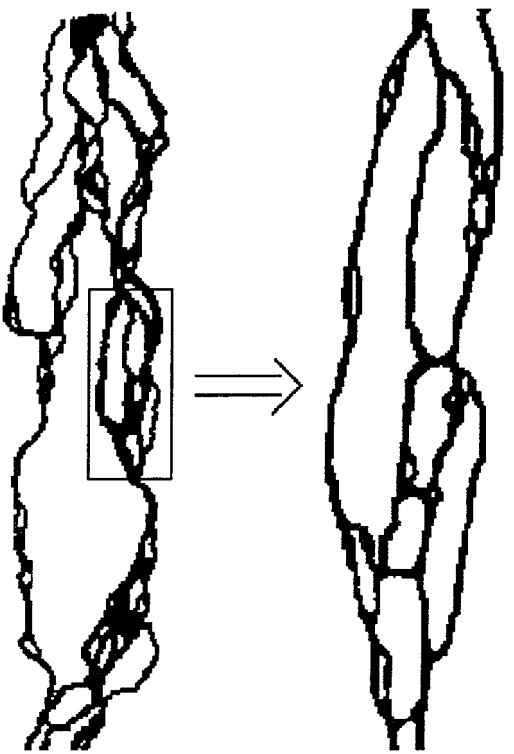

Figure 1. Illustration of anisotropic scaling in the morphology of a braided river (the Hulahula River in Alaska). A small part of the river (the one enclosed within the rectangle) was enlarged by stretching its horizontal axis by a factor of 2.5 and its vertical axis by a factor of $(2.5)^{1.5} \cong 4$. The stretched small part of the river looks statistically similar to the original larger part.

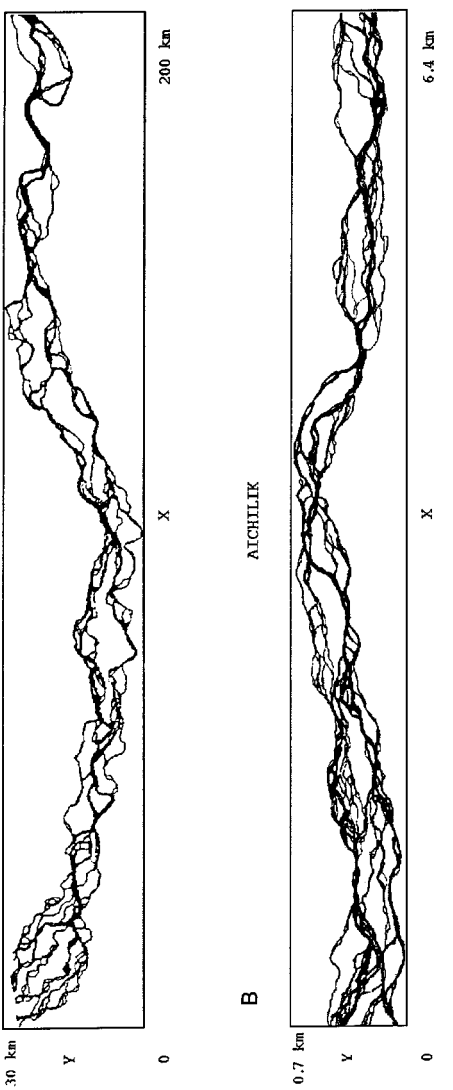

Figure 2. The digitized images of A, the Brahmaputra River (Bangladesh), B, the Aichilik River (Alaska), and C, the Hulahula River (Alaska).

by visual comparison of their spatial patterns. This leads one to believe that, at least qualitatively, there are statistical similarities and scale invariances among parts of different size of a single braided river and between one braided river and another.

In our previous work (Sapozhnikov and Foufoula-Georgiou, 1995; Sapozhnikov and Foufoula-Georgiou, 1996a,b) the mathematical tools necessary to quantify these similarities and scale invariances were developed and applied to a suite of digitized braided rivers from areal photographs or synthetic aperture radar (SAR) imagery (e.g., Nykanen, Foufoula-Georgiou, and Sapozhnikov, 1998). Quantification of these statistical scale invariances provides a formal way of studying similarities and differences in the morphology of braided rivers of different hydrogeologic characteristics. It is believed that the presence of scale invariances is an indication of the presence of universal features in the underlying physical mechanisms responsible for the formation of the spatial structure of braided rivers. Indeed, it was found (Nykanen, Foufoula-Georgiou, and Sapozhnikov, 1998) that if the braided river systems were not free of external topographic controls, e.g., when predominant geologic controls such as mountains or predominant flow paths were present, scale invariance was absent.

Braided rivers, besides their complex geometry at any instant of time, are also highly dynamic systems characterized by intensive erosion, sediment transport and deposition, and frequent channel shifting as they evolve. Understanding and statistically quantifying the evolution of braided rivers has important applications in hydraulic structure planning and environmental exploration, which depend on quantifying the frequency and magnitude of channel shifting. It is also important in investigating links between the physical mechanisms controlling the evolution of these systems at a range of scales and the statistical structure of the resulting braided river patterns. A framework under which morphology and evolution of braided rivers can be studied simultaneously at a range of scales was developed in Sapozhnikov and Foufoula-Georgiou (1997). Application of this framework to an experimentally produced braided river revealed interesting space–time relations and provided insight on the self-organization of these highly complex natural systems which seem to bring themselves, by horizontal and vertical adjustments, to a statistical equilibrium state that is also a critical state for the system (e.g., Sapozhnikov and Foufoula-Georgiou, 1999).

This paper presents an overview of the philosophy and methodologies needed to quantify the morphology and evolution of braided rivers. It also presents a summary of the results of applying these methodologies to a variety of natural and experimental braided rivers. It concludes with a discussion of future research directions and the still remaining challenge of understanding and quantifying not only the geomorphologic but also the hydrologic behavior of braided rivers at a range of spatiotemporal scales.

HOW TO QUANTIFY SELF-AFFINITY?

The presence of spatial scaling in an object means that statistical properties at one scale relate to statistical properties at another scale via a transformation that involves only the ratio of the two scales. This is also known as "scale invariance" and means that the object is statistically indistinguishable under proper magnification or contraction. When the properties scale similarly in all directions, it is referred to as "isotropic scaling," and the object is a self-similar fractal. However, when the properties scale differently in different directions, it is called "anisotropic scaling," and the object is a self-affine fractal. Sapozhnikov and Foufoula-Georgiou (1995) developed a methodology to test and quantitatively assess the presence of self-affinity in any complex geometrical pattern, such as a braided river, and to estimate the fractal exponents that define its spatial scaling. This method is called the "logarithmic correlation integral (LCI) method," and is briefly presented here for completeness.

Let X and Y be the sides of a rectangle and $M(X, Y)$ be the mass (e.g., the number of pixels covered by water) of the part of the object contained within the $X \times Y$ rectangle. Then, spatial scaling implies that

$$M(X, Y) \sim X^{1/\nu_x} \sim Y^{1/\nu_y} \tag{1}$$

where ν_x and ν_y are the fractal exponents corresponding to the X and Y directions, respectively. Note that according to Equation (1), the mass $M(X, Y)$ scales with the sides of the rectangle only if X scales with Y in a certain way. Equation (1) can be written in the form

$$\left(\frac{X_2}{X_1}\right)^{1/\nu_x} = \left(\frac{Y_2}{Y_1}\right)^{1/\nu_y} = \left(\frac{M_2}{M_1}\right) \tag{2}$$

If we introduce $x = \log X$, $y = \log Y$, and $z = \log M$, we get

$$\frac{x_2 - x_1}{\nu_x} = \frac{y_2 - y_1}{\nu_y} = z_2 - z_1 \tag{3}$$

or

$$\frac{dx}{\nu_x} = \frac{dy}{\nu_y} = dz \tag{4}$$

The function $M(X, Y)$ is known as the correlation integral, and by analogy we call the function $z(x, y)$ the "logarithmic correlation integral" of the object under study. Comparing Equation (4) with

$$\frac{\partial z}{\partial x}dx + \frac{\partial z}{\partial y}dy = dz \tag{5}$$

we obtain

$$\nu_x \frac{\partial z}{\partial x} + \nu_y \frac{\partial z}{\partial y} = 1 \tag{6}$$

This relationship provides a method for testing the presence of spatial scaling and for estimating the fractal exponents ν_x and ν_y of a self-affine object, as follows. Having estimated the logarithmic correlation integral $z(x, y)$ from a pattern of the object by direct calculation of the mass $M(X, Y)$ (i.e., pixels covered by water) within rectangles of sizes $X \times Y$, one can calculate the derivatives $\partial z(x, y)/\partial x$ and $\partial z(x, y)/\partial y$ and use them to test whether the linear relationship [Eq. (6)] is satisfied and, if yes, to find the values of ν_x and ν_y. As can be seen from the above equation, $1/\nu_y$ is the intercept of the linear best fit line with the vertical axis, and $-\nu_x/\nu_y$ is the slope. Ideally, only two points are needed to estimate ν_x and ν_y, but for a good estimation a least squares fit to the derivatives at all points of the surface $z(x, y)$ is preferable. Since both coordinates contain uncertainty in their values, it is not appropriate to use the traditional least squares method. This method minimizes the sum of the squares of the vertical distances between the fitted line and the actual data points and is sensitive to the orientation of the coordinate system. Thus, another method that minimizes the sum of the squares of the perpendicular to the best-fit line distances was used. This method was implemented with the revised algorithm of Alciastore and Miranda (1995), which is numerically stable and gives a unique solution.

EVIDENCE OF SELF-AFFINITY IN BRAIDED RIVERS

The method described in the previous section was applied to several natural braided rivers: the Brahmaputra River (Bangladesh), the Aichilik and Hulahula Rivers (Alaska), and several reaches of the Tanana River (Alaska). Details about the geological and hydrological settings of these rivers as well as details of the tracing and digitization of the air and satellite images can be found in Sapozhnikov and Foufoula-Georgiou (1996a,b) and Nykanen, Foufoula-Georgiou, and Sapozhnikov (1998).

Figure 3 shows the partial derivatives of the correlation integral surfaces $z(x, y)$, i.e., the plots $\partial z/\partial x$ vs. $\partial z/\partial y$ for the three braided rivers shown in Figure 2. The points on the plots show a good linear dependence indicating the presence of self-affinity in all three rivers. The values of the scaling exponents ν_x and ν_y were estimated, and were found to be very close to each other for all three rivers: $\nu_x = 0.74$ and $\nu_y = 0.51$ for Brahmaputra; $\nu_x = 0.72$ and $\nu_y = 0.51$ for Aichilik; and $\nu_x = 0.74$ and $\nu_y = 0.52$ for Hulahula.

The same methodology was applied to several segments of the Tanana River in Alaska extracted from ERS-1 (European Remote Sensing Satellite) SAR imagery

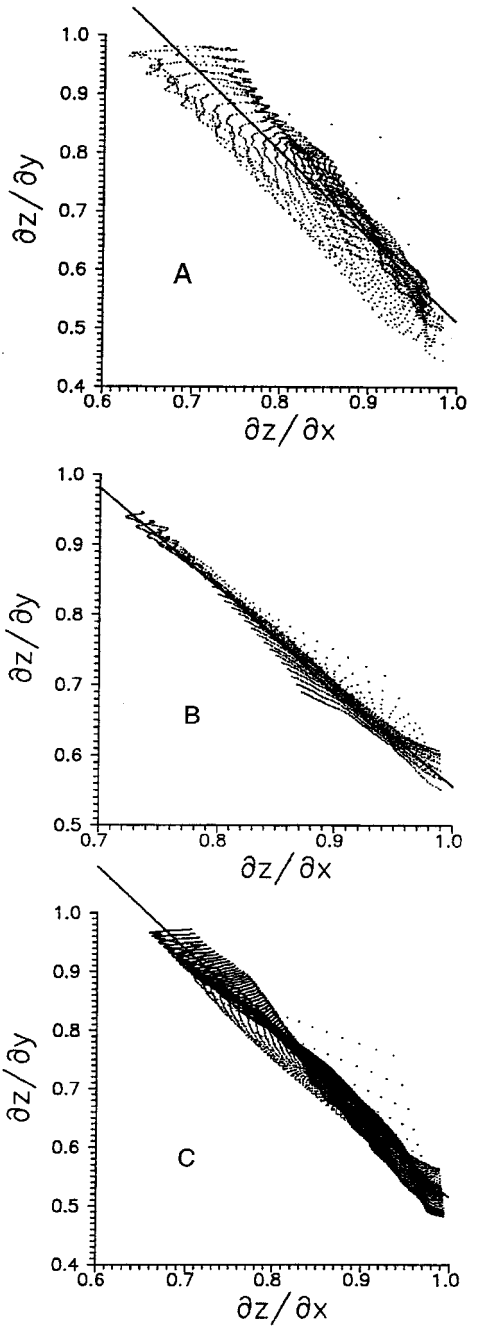

Figure 3. Evidence for the presence of self-affinity and estimation of the fractal exponents ν_x and ν_y for the A, Brahmaputra, B, Aichilik, and C, Hulahula Rivers.

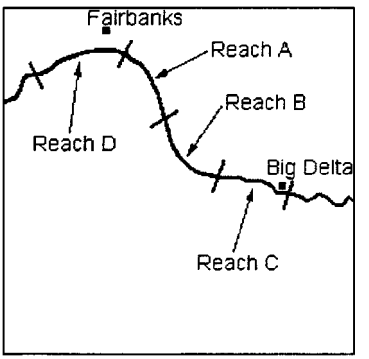

Figure 4. Reaches of the Tanana River studied for the presence of self-affinity. The lengths of the reaches A, B, C, and D are 28.6, 34.2, 25.8, and 32.2 km, respectively.

(Fig. 4). Pictures of the satellite images of these reaches are shown in Figure 5. For the details of the extraction methodology, see Nykanen, Foufoula-Georgiou, and Sapozhnikov (1998). Figure 6 shows the $\partial z/\partial y$ vs. $\partial z/\partial x$ plots for the four reaches of the Tanana River. Good scaling is observed in reach A; moreover the scatter of points around the best-fit straight line is similar to the scatter found for the three previous rivers in Figure 3. However, the plots for reaches B and C of the Tanana River display relatively poor scaling and the clouds of points are different from those of the typical curves. In both Figures 5B and 5C the main body of the cloud takes on a concave shape, and the cloud lacks the fullness and even distribution of points throughout its mass. The reason for this poor scaling might be the interaction of the physical mechanisms controlling the braid plain morphology with external factors imposed on the rivers. In both reaches B and C, a mountainous region adjacent to the river affected strongly the path of the river. When the braid plain of a river reach is forced by an external factor, it is definitely other mechanisms besides braiding that control the resulting morphology of the river. It appears that the prerequisite for spatial scaling is that the river is allowed to evolve in a natural, self-organized way such that the spatial structure of the river is determined by the same mechanisms at all scales. Any interference with this self-organization can break the underlying spatial scaling. Indeed, large-scale perturbations caused by external factors (e.g., mountains) are shown here to affect the scaling properties of the river pattern at all scales (even scales smaller than the scale of the external factor). (See Nykanen, Foufoula-Georgiou, and Sapozhnikov, 1998 for more explanation.)

Reach D, located downstream of Fairbanks, is different from the other reaches in that the slope is more gradual and the braiding index is lower (3.14 compared to 4.59, 4.23, and 5.22 for the other reaches). The SAR image of this reach for the July 8, 1993, scene is shown in Figure 5D. Although no morphological constraints seem present, the reach is characterized by braiding with a predominant channel throughout its length. The width of this main channel is only 4 times

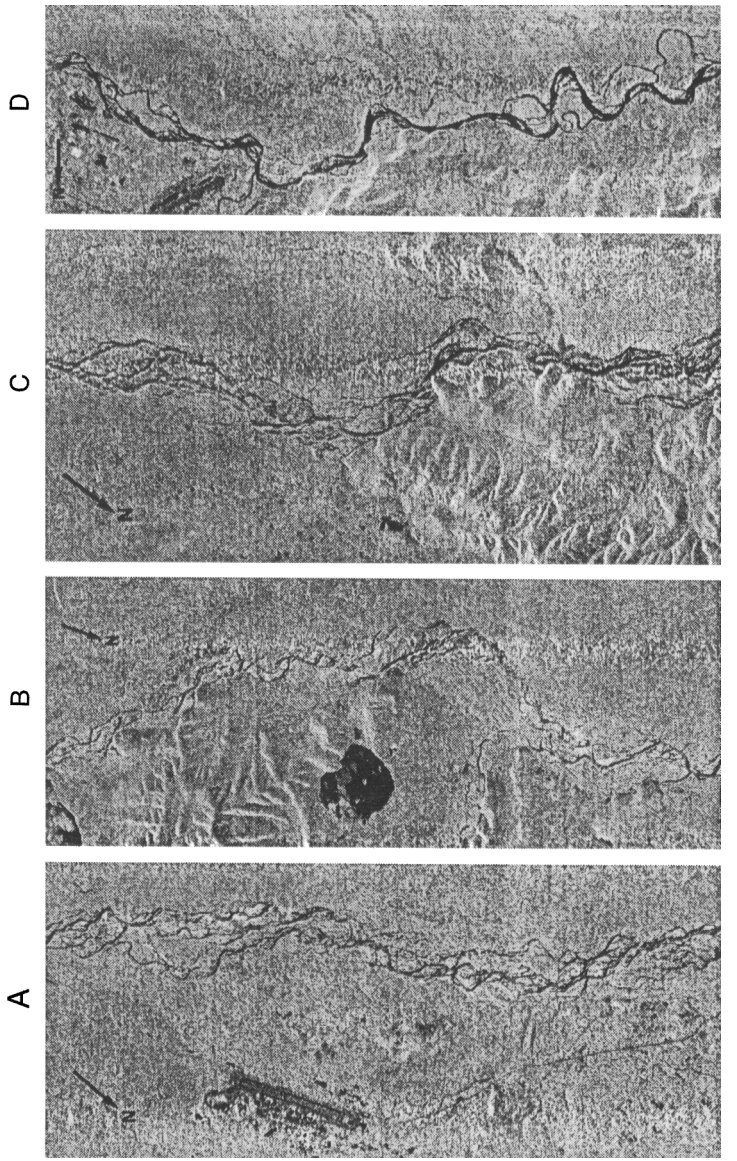

Figure 5. SAR images for reach A (May 31, 1993; flow rate 35,300 cfs); reach B (May 31, 1993; flow rate 35,300 cfs); reach C (July 2, 1993; flow rate 51,300 cfs), and reach D (July 8, 1993; flow rate 49,100 cfs).

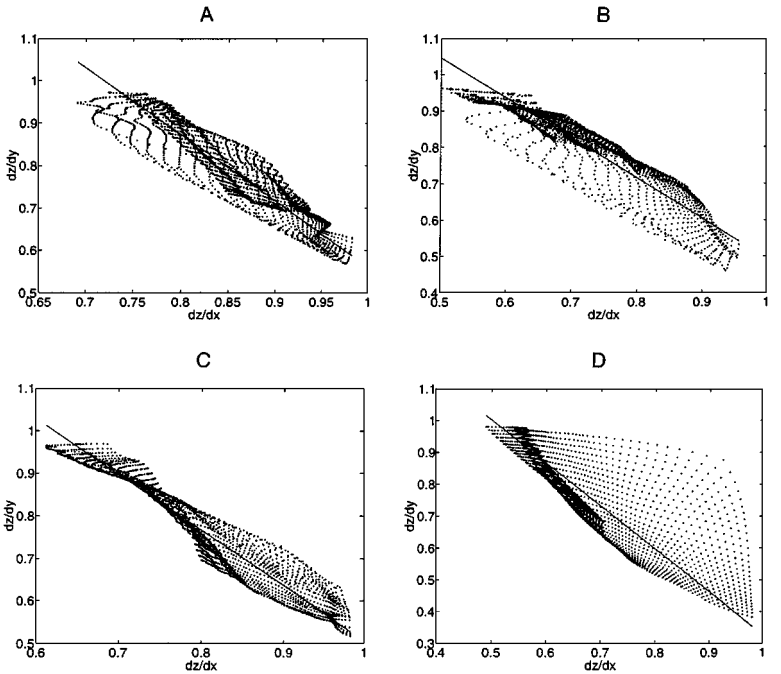

Figure 6. Testing the presence of spatial scaling and estimation of the fractal exponents ν_x and ν_y for the extracted braided river patterns of the Tanana River: A, reach A, B, reach B, C, reach C, and D, reach D.

smaller than the whole braid plain width and approximately 10 times larger than the next biggest channel; that is, channels of intermediate widths are missing from this river reach. Our analysis showed (see Figure 6D) that such rivers, which are braided but have a predominant channel, do not exhibit self-affine scaling. It should be also noted that reach D is geographically a transitional river reach, connecting a fully braided regime (with all scales of channel present) to a single meandering river regime.

It is interesting to point out that fully developed braided rivers were found to form a class of scale-invariant objects which lie between the classes of single-channel rivers and river networks (see Table 2). The scaling anisotropy of braided rivers (characterized by the ν_x/ν_y value) is lower than that of the single-channel rivers but higher than that of river networks. Also, the global fractal dimension $D_G = (\nu_y - \nu_x + 1)/\nu_y$ (see Mandelbrot, 1986, or Sapozhnikov and Foufoula-Georgiou, 1996a,b) shows that braided rivers fill the surface more densely than single-channel rivers but not as densely as river networks.

Table 2. Average Fractal Characteristics of Single-Channel Rivers, River Networks, and Braided Rivers

Objects	ν_x	ν_x	ν_x/ν_x	D_G
Single-channel rivers[a]	∼1	∼0.5	∼2	∼1
River networks[b]	0.62	0.47	1.32	1.83
Braided rivers[c]	0.75	0.51	1.43	1.52

[a] Reaches of the Dniester and Pruth Rivers in Moldova (Nikora, Sapozhnikov, and Noever, 1993).
[b] Sixty river networks (Nikora and Sapozhnikov, 1993; Nikora, 1994).
[c] This study.

HOW TO QUANTIFY SPATIOTEMPORAL SCALE INVARIANCE?

Spatial scaling in a fractal object implies that the object looks statistically the same at different spatial scales. If, additionally, it evolves in such a way that after a proper rescaling of time its evolution is also statistically indistinguishable at different scales, then we say that in addition to spatial scaling, the object exhibits dynamic scaling. The space–time rescaling has the form

$$\frac{t_2}{t_1} = \left(\frac{L_2}{L_1}\right)^z \tag{7}$$

where L_1 and L_2 are the scales at which the evolution of the object is considered, t_2/t_1 is the time rescaling factor, and z is called the dynamic scaling exponent. One can see Equation (7) as providing the space–time rescaling needed to have the projection of the evolution of part $L_1 \times L_1$ on a screen, statistically indistinguishable from the projection of part $L_2 \times L_2$ on a screen of the same size.

Let us characterize the evolution of a stationary fractal object by "changes" in its pattern, where changes are defined as parts of the space that were not occupied by the object at a certain moment of time but became occupied after some time lag t. Let $n(l' > l, t)$ denote the number of changes exceeding size l after some time lag t, and D be the fractal dimension of the object (e.g., in this work it is the fractal dimension of the braided river spatial pattern). It can be shown (Sapozhnikov and Foufoula-Georgiou, 1997) that the condition for dynamic scaling (7) can be written in terms of the statistics of changes as

$$n(l' > l, t) = l^{-D} f\left(\frac{t}{l^z}\right) \tag{8}$$

where $f(\cdot)$ is some function.

For time lag $t = 0$ there are no changes in the object, which implies $n(l' > l, 0) = 0$, and correspondingly, that $f(0) = 0$. If for small values of the argument, the function f can be approximated by a power law, with some exponent β, then the condition (8) for dynamic scaling takes the form

$$n(l' > l, t) \sim t^{\beta} l^{-D-\beta z} \tag{9}$$

Although, in contrast to Equation (8), Equation (9) holds only for small values of t/l^z, it can be conveniently used to facilitate the estimation of the dynamic scaling exponent z. Indeed, the following procedure of estimating z was employed in Sapozhnikov and Foufoula-Georgiou (1997). It was based on their empirical finding that in the experimental braided river, at small t/l^z values

$$n(l' > l, t) \sim l^{-k} \tag{10}$$

for every fixed value of the time lag t, and

$$n(l' > l, t) l^k \sim t^{\beta} \tag{11}$$

for every fixed value of l. These two equations coincide with Equation (9), with the dynamic exponent z given as

$$z = (k - D)/\beta \tag{12}$$

Thus, in a system showing dynamic scaling one can first estimate the k exponent from the log–log plots of $n(l' > l, t)$ vs. l (for several fixed values of t) and the β exponent from the log–log plot of $n(l' > l, t) l^k$ against t. This, together with the fractal dimension D of the system (estimated using, for example, the mass-in-a-box method; Mandelbrot, 1982) enables estimation of z using Equation (12). Then one can plot for the estimated value of z, the value of $n(l' > l, t) l^D$ vs. t/l^z, for all (and not only small) values of t/l^z, to verify that the general equation of dynamic scaling [Eq. (8)] holds. Collapsing of all curves to a single curve, the $f(\cdot)$ curve in [Eq. (8)], would verify the presence of dynamic scaling in the river. The procedure is schematically displayed in the diagram of Figure 7.

It is noted that the methodology presented in this section follows the approach of Sapozhnikov and Foufoula-Georgiou (1997) that does not include dynamic scaling anisotropy. The reader is referred to the more elaborate methodology developed in Foufoula-Georgiou and Sapozhnikov (1998), which allows detection of dynamic scaling anisotropy in evolving complex objects.

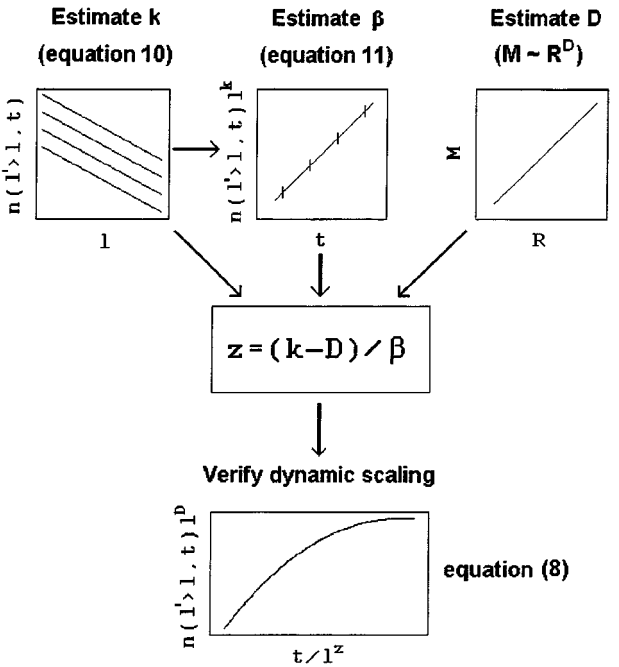

Figure 7. Schematic of estimation and verification procedure for dynamic scaling.

EVIDENCE OF DYNAMIC SCALING IN BRAIDED RIVERS

The procedure outlined in the previous section and summarized schematically in Figure 7 can be used to test the presence of dynamic scaling in an evolving (spatially changing over time) braided river system. Since observations of the evolution of natural braided rivers are very difficult to obtain from *in situ* field measurements and the resolution of satellite images is not high enough to capture the evolution of these rapidly changing systems, a braided river system was experimentally produced in the laboratory and monitored at high spatial and temporal resolution. Details of the experimental setup can be found in Sapozhnikov and Foufoula-Georgiou (1997). The experimental basin was 5×0.75 m and was continuously supplied with sediment (grain size $= 0.12 \pm 0.03$ mm with discharge rate of 0.6 g/sec) and water (discharge rate of 20 g/sec). A video camera recorded the evolution of the system. To visualize the river and monitor its depth, dye was supplied continuously during each videotaping session. After each videotaping session, the dye supply was cut and water flushed the dye from the system in a matter of a few hours. The recorded data were consequently digitized for treatment and analysis. The studied region size was 0.75×1.0 m and was located between

the 2.8 and 3.8 m marks (measured from the point of inflow). The final resolution of images was 3 mm across the river and 1.5 mm along the river.

The cumulative probability distributions of the sizes of changes (characterized by the square root of their areas) were estimated for time lags of 3, 4, 5, 7, 9 and 15 sec and are shown in Figure 8A. As can be seen from this figure, these distributions can be well approximated by power laws for different time lags, and the slopes of the log–log plots of the distributions are very close to each other giving an estimate of $k = 2.8$. The log–log plot of $n(l' > l, t)l^k$ against t shown in Figure 8B suggests a power law dependence and gives an estimate of β equal to 2.0. These estimates of k and β together with an estimate of $D = 1.75$ (see Sapozhnikov and Foufoula-Georgiou, 1997) give an estimate of the dynamic scaling exponent $z \cong 0.5$. The plot of the rescaled distributions is shown in Figure 8C. It is observed that all curves (rescaled probability distributions) collapse to a single curve providing full evidence for the presence of dynamic scaling.

The physical interpretation of the value of the dynamic scaling exponent was extensively discussed in Sapozhnikov and Foufoula-Georgiou (1997). Comparing the obtained estimate of $z \cong 0.5$ with the value of $z = 2$ (i.e., lifetime of channels would be controlled by a diffusion-type process and would be proportional to the square root of the spatial scale) and the value of $z = 0$ (no rescaling would be needed going from a small to a larger spatial scale; i.e., lifetime of channels of all widths would be the same), it was concluded that a strong correlation exists between the evolution of large and small channels within a braided river system. More specifically, it was conjectured that the evolution of small channel patterns is to a great extent forced by the evolution of larger channels (see Sapozhnikov and Foufoula-Georgiou, 1997).

In addition to revealing spatial and temporal scaling relationships that allow one to describe the morphology and evolution of braided rivers, it is very important to get insight into the mechanisms responsible for these features. In Sapozhnikov and Foufoula-Georgiou (1998, 1999), it was shown that the mechanism bringing braided rivers to a state where they show spatial and temporal scaling is self-organized criticality (SOC). This conclusion was based on the known facts that braided rivers (1) are nonlinear systems, (2) have a large number of degrees of freedom, and (3) show collective behavior that is a crucial feature of systems at a critical state; and on our findings that braided rivers (1) exhibit spatial scaling, (2) exhibit dynamic scaling at the critical state, and (3) dynamic scaling emerges only as they approach the critical state and is not present before this state is reached.

DISCUSSION AND CONCLUSIONS

Braided river systems manifest themselves over a large range of scales, e.g., from the smallest channels of a few meters to the whole braid plain width of tens of kilometers. Understanding how morphological and dynamical properties of the

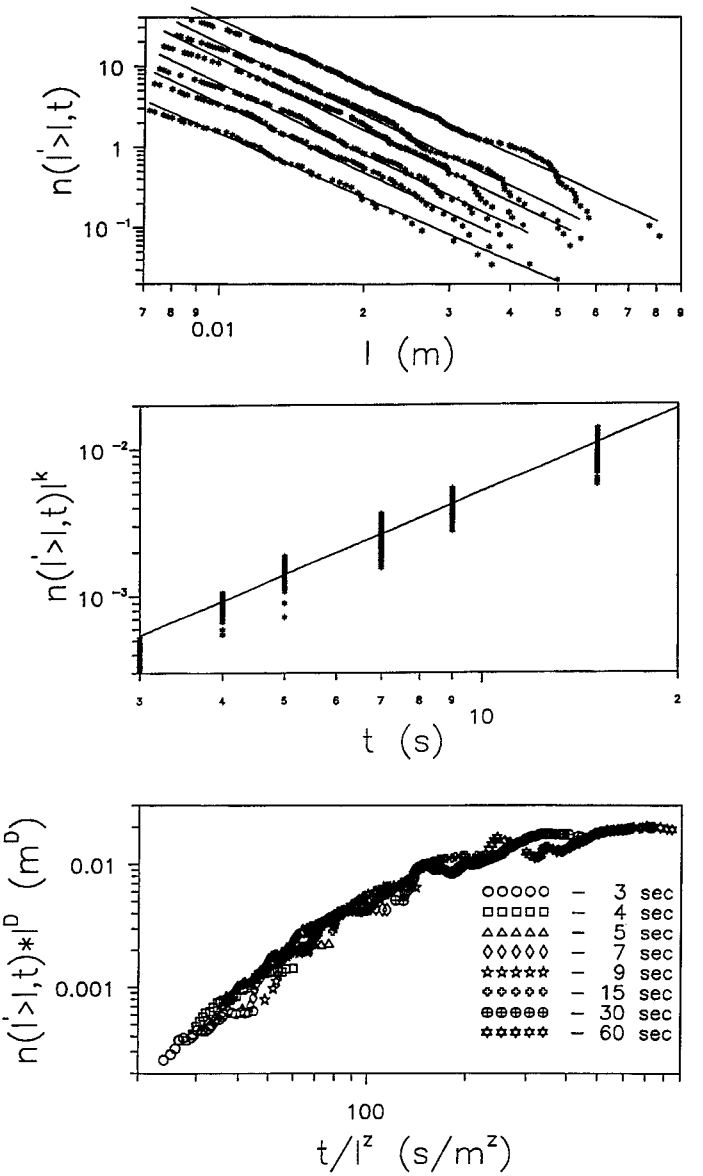

Figure 8. Evidence of dynamic scaling in the experimental braided river following the procedure illustrated in Figure 7. In the top figure, empirical (points) and straight-line fitted pdfs are for time lags of 3, 4, 5, 7, 9, and 15 s from bottom to top.

system at one scale relate to those at another scale is essential when applying the knowledge gained from a small part of a braided river to a larger part of it, from one braided river to another of different size, or from a laboratory model to a real braided river.

From our analysis of real and experimental braided rivers, it was concluded that space and time can be appropriately rescaled such that the morphology and evolution of parts of a braided river of different size would be statistically indistinguishable. This statistical scale invariance within parts of the same river and the similarity of the scaling exponents from one river to another was interpreted as indicating the presence of universal features in the underlying mechanisms responsible for the formation of braided rivers. Also the dynamic scaling relationships can be used to statistically predict long-term extreme changes of the system at a large spatial scale (for which not many data are available) from short-term frequent changes at a smaller spatial scale (which can be easily monitored).

It is emphasized that our dynamic analysis compared small and larger parts of one river system and not of one system with another. The latter would require inclusion of other physical parameters that govern the evolution of rivers. For example, slope plays a crucial role in the rate of river evolution (the greater the slope, the faster the evolution). Other important factors are the type of sediment and the total water and sediment flux in a river (the greater the imposed flux, the faster the evolution) (Ashmore, 1985). To relate the rate of evolution of different braided stream systems, Equation (7) has to be extended. Sapozhnikov and Foufoula-Georgiou (1997) conjectured that under the scaling hypothesis, Equation (7) would take the form:

$$\frac{t_2}{t_1} = \left(\frac{L_2}{L_1}\right)^z \left(\frac{S_2}{S_1}\right)^\gamma \cdots \tag{13}$$

where S is the slope of a river and the dots imply that other parameters could enter this equation in a power-law multiplicative way. Toward developing the precise form of Equation (13), study through laboratory experiments of the effect of the sedimentological and hydrological characteristics (slope, input water and sediment discharge, and grain size) on the evolution and scaling exponents of braided rivers is needed. Such a study is currently underway in our laboratory.

Also, in our analysis, the evolution of the braided river system has been characterized by the projection of changes on a horizontal plane, although changes in a river are truly three-dimensional structures. In other words, any areas that became deeper, shallower, covered by water or exposed were treated in the same way and their horizontal projections formed the “changes” that characterized the river evolution. A more detailed analysis that includes consideration of the depth of changes in addition to their horizontal sizes would be of interest as it would characterize the hydrology in addition to the morphology of braided rivers. Such data

of depth changes are difficult to collect but current procedures at the St. Anthony Falls Laboratory have allowed us to do so. Further research will include the study of the hydrologic dynamics of braided rivers at a range of spatiotemporal scales.

ACKNOWLEDGMENTS

This research was supported by NSF grant EAR-9628393 and NASA grant NAG5-6191. We thank our research collaborators Chris Paola, Deborah Nykanen, and Brad Murray, whose ideas contributed significantly in integrating and advancing our understanding of braided rivers. ERS-1 data were acquired by the European Space Agency and were provided by NASA through the Alaska SAR facility. The Minnesota Supercomputer Institute (MSI) was generous in providing computer facilities for our research.

REFERENCES

Alciatore, D., and Miranda, R., 1995, The best least-squares line fit, *in* Paeth, V. A. W., ed. Graphics Gems: Academic, San Diego, CA, p. 91–97.

Ashmore, P., 1985, Process and form in gravel braided streams: Laboratory modelling and field observations, unpubl. doctoral dissertation, University of Alberta, Edmonton.

Ashmore, P., and Parker, G., 1983, Confluence scour in coarse braided streams: Water Resour. Res., v. 19, p. 392–402.

Ashmore, P. E., Ferguson, R. I., Prestegaard, K. L., Ashworth, P. J., and Paola, C., 1992, Secondary flow in anabranch confluences of a braided, gravel-bed stream: Earth Surf. Processes Landforms, v. 17, p. 299–311.

Best, J. L., 1986, The morphology of river channel confluences: Prog. Phys. Georgr., v. 10, p. 157–174.

Bristow, C., and Best, J., 1993, Braided rivers: Perspectives and problems, *in* Best, J., and Bristow, eds., Braided Rivers: Geological Society, London, p. 1–11.

Bristow, C. S., Best, J. L., and Roy, A. G., 1993, Morphology and facies models of channel confluences, *in* Marzo, M., and Puigdefabregas, C., eds., Alluvial Sedimentation: Blackwell Scientific, Cambridge, MA, p. 91–100.

Foufoula-Georgiou, E., and Sapozhnikov, V., 1998, Anisotropic scaling in braided rivers: An integrated theoretical framework and results from application to an experimental river: Water Resour. Res., v. 34, no. 4, p. 863–867.

Howard, A. D., Keetch, M. E., and Vincent, C. L., 1970, Topological and geometrical properties of braided streams: Water Resour. Res., v. 6, p. 1674–1688.

Mandelbrot, B. B., 1982, The Fractal Geometry of Nature: W. H. Freeman, New York.

Mandelbrot, B. B., 1986, Self-affine fractal sets, in Fractals in Physics, *in* Petroniero, L., and Tosatti, E., eds., Proceedings of the Sixth Trieste International Symposium on Fractals in Physics, ICTP, Trieste, Italy: North-Holland, New York, p. 3–16.

Mosley, M. P., 1976, An experimental study of channel confluences: J. Geol., v. 84, p. 535–562.

Mosley, M. P., 1977, Stream junctions: A probable location for bedrock placers: Econ. Geol., v. 72, p. 691–697.

Murray, A. B., and Paola, C., 1994, A cellular model of braided rivers: Nature, v. 371, p. 54–57.

Nikora, V. I., 1994, On self-similarity and self-affinity of drainage basins: Water Resour. Res., v. 30, p. 133–137.

Nikora, V. I., and Sapozhnikov, V. B., 1993, River network fractal geometry and its computer simulation: Water Resour. Res., v. 29, p. 3569–3575.

Nikora, V. I., Sapozhnikov, V. B., and Noever, D. A., 1993, Fractal geometry of individual river channels and its computer simulation: Water Resour. Res., v. 29, p. 3561–3568.

Nykanen, D., Foufoula-Georgiou, E., and Sapozhnikov, V., 1998, Study of spatial scaling in braided river patterns using synthetic aperture radar imagery: Water Resour. Res., v. 34, no. 7, p. 1795–1807.

Robert, A., 1993, Bed configuration and microscale processes in alluvial channels: Prog. Phys. Geogr., v. 17, p. 123–136.

Sapozhnikov, V., and Foufoula-Georgiou, E., 1995, Study of self-similar and self-affine objects using logarithmic correlation integral: J. Phys. A: Math. Gen., v. 28, p. 559–571.

Sapozhnikov, V., and Foufoula-Georgiou, E., 1996a, Do the current landscape evolution models show self-organized criticality? Water Resour. Res., v. 32, no. 4, p. 1109–1112.

Sapozhnikov, V., and Foufoula-Georgiou, E., 1996b, Self-affinity in braided rivers: Water Resour. Res., v. 32, no. 5, p. 1429–1439.

Sapozhnikov, V., and Foufoula-Georgiou, E., 1997, Experimental evidence of dynamic scaling and indications of self-organized criticality in braided rivers: Water Resour. Res., v. 33, no. 8, p. 1983–1991.

Sapozhnikov, V., Brad Murray, A., Paola, C., and Foufoula-Georgiou, E. 1998, Validation of braided-stream models: Spatial state-space plots, self-affine scaling, and island shapes: Water Resour. Res., v. 34, no. 9, p. 2353–2364.

Sapozhnikov, V., and Foufoula-Georgiou, E., 1999, Horizontal and vertical self-organization of braided rivers toward a critical state: Water Resour. Res., v. 35, no. 3, p. 843–851.

Smith, L. C., Isacks, B. L., Forster, R. R., Bloom, A. L., and Presuss, I., 1995, Estimation of discharge from braided glacial rivers using ERS 2 synthetic aperture radar: First results: Water Resour. Res., v. 31, p. 1325–1329.

Smith, L. C., Isacks, B. L., Bloom, A. L., and Murray, A. B., 1996, Estimation of discharge from three braided rivers using synthetic aperture radar satellite imagery: Potential applications to ungaged basins: Water Resour. Res., v. 32, p. 2031–2034.